

# Current–voltage curves for molecular junctions: the issue of the basis set for the metal contacts

Charles W. Bauschlicher Jr. · John W. Lawson

Received: 31 August 2007 / Accepted: 7 November 2007 / Published online: 27 November 2007  
© Springer-Verlag 2007

**Abstract** We present current–voltage ( $I$ – $V$ ) curves for a chain of six Au atoms and for benzene-1,4-dithiol between two Au (111) surfaces computed using a self-consistent, non-equilibrium, Green’s Functions approach in conjunction with a density functional theory (DFT) description of the extended molecule. The solutions are expanded in Gaussian basis sets. In an attempt to improve the description of the molecule–surface bond, we consider one- and two-layer clusters of metal atoms in the extended molecule. To avoid non-physical charging of the bulk metal clusters we add a shift to the diagonal elements of the Fock Matrix of the metal atoms in the DFT treatment; this can be viewed as correcting the self-energies or shifting the Fermi level. The Au<sub>6</sub> cluster with the full minimal basis set represents a compromise between accuracy and cost. The Au<sub>31</sub>(12/19) two-layer cluster results are of about the same quality as the one-layer Au<sub>21</sub> cluster, but allows one to study more binding sites. Using a double zeta basis set for three of the top-layer Au atoms of the Au<sub>31</sub>(12/19) cluster yields result similar to the all minimal basis set, while using all double zeta atoms yields inferior results.

**Keywords** DFT · Greens Functions · Current–voltage curves · Molecular electronics

## 1 Introduction

Several programs [1–10] have been developed to compute current–voltage ( $I$ – $V$ ) curves for molecular junctions. While

the different codes have many similarities, they also have many differences, and, at the present time, it is not clear as to the best method for the calculation of  $I$ – $V$  curves. In the approach that we are using, the bridging molecule and some metal atoms from each metal surface are treated as an extended molecule that are coupled to the two semi-infinite electrodes. The coupling between the bulk contacts and the extended molecule is determined at the tight-binding level [11] using a metal cluster that includes the metal atoms in the extended molecule and all of its neighbors in the first and second layers. The effect of all other layers is accounted for using a recursive Green’s function procedure which is performed once during the calculation of the self-energies.

Recently we showed [12] that the approach we use correctly predicted a reduction in the current flow with the addition of electron withdrawing substituents, an effect that other approaches have missed. While the approach we use has many desirable features, it also has some limitations. Since we are explicitly treating only one layer of the metal atoms, we are unable to model the difference between a hollow site on a (111) face with and without an atom in the second layer. In addition, since the tight-binding self-energies are mapped onto the basis functions in the density functional theory (DFT) description of the extended molecule, only a minimal basis set can be used for the metal atoms in the extended molecule that are coupled to the bulk. While minimal basis sets are expected to capture the qualitative features of the bonding, often larger basis sets are required to accurately describe the bonding. Thus it is desirable to move beyond the single layer of metal atoms described using only a minimal basis set.

As has been previously noted [13], using a minimal metal set that was optimized for the free Au atom leads to nonphysical charging of the metal atoms in the extended molecule. It has been found that it is possible to avoid most of the charg-

C. W. Bauschlicher Jr. (✉) · J. W. Lawson  
Mail Stop 230-3, Center for Advanced Materials and Devices,  
NASA Ames Research Center, Moffett Field, CA 94035, USA  
e-mail: Charles.W.Bauschlicher@nasa.gov

J. W. Lawson  
e-mail: John.W.Lawson@nasa.gov

ing by removing the most diffuse s, p, and d basis functions from the metal basis set. Because the basis set convergence is more rapid for a description of the solid than for the description of a molecule, the diffuse functions are less important for the description of a solid, which permits the truncation while still giving a reasonable description of the surface. This basis set truncation for the solid is supported by optimization of the basis set for a metal cluster, where the diffuse functions are much more contracted than those found in basis sets optimized for the metal atoms [14]. In other words, the diffuse functions from the atom optimization are not suited for the treatment of the solid. After truncation of the basis set, some small charging of the explicit metal atoms still occurs even when no bridging molecules are present. In the previous work, the metal cluster was made completely neutral by adding a small shift to the DFT Hamiltonian elements associated with the metal basis functions, i.e.  $\text{shift} \times S$  (metal basis functions only), where  $S$  is the overlap matrix.

We are investigating several extensions to the approach that we use to treat the solid, for example, replacing the tight binding with a DFT treatment and extending our treatment of the solid to include more than one layer of metal atoms in the extended molecule with all of the layers coupled to the bulk. In this work we consider a simplified approach where we continue to have only one layer of metal atoms coupled to bulk, but add a second layer of atoms on top of those coupled to the bulk. This approach allows the use of an arbitrary basis set on the top layer, but larger basis sets can lead to nonphysical charging, as found previously. Therefore, in addition to studying two layers, we also address the question of adding a shift to the metal atoms in the DFT Hamiltonian to eliminate any unwanted charging even if the shift becomes large for some basis sets. We use two systems to test our extensions: a chain of six Au atoms between two Au(111) surfaces and benzene-1,4-dithiol between two Au(111) surfaces.

## 2 Methods

We use the same basic approach as described in previous work, namely, the  $I-V$  curves are computed using the self-consistent, non-equilibrium, Green's function approach as implemented by Xue, Datta, and Ratner [1, 15–18], but modified for the hybrid integration [19]. Using this approach, the bridging molecule is described using an all-electron basis set, while the contacts are described using an effective core potential (ECP). We consider two systems that we have studied previously [14, 20] and the reader is referred to the original work for more details. The first system is a chain of six Au atoms between two Au(111) surfaces, while the second system is benzene-1,4-dithiol between two Au(111) surfaces.

In both sets of calculations, a cluster of metal atoms from each metal surface is included in the extended molecule calculation. The geometries of the Au atoms in the clusters used

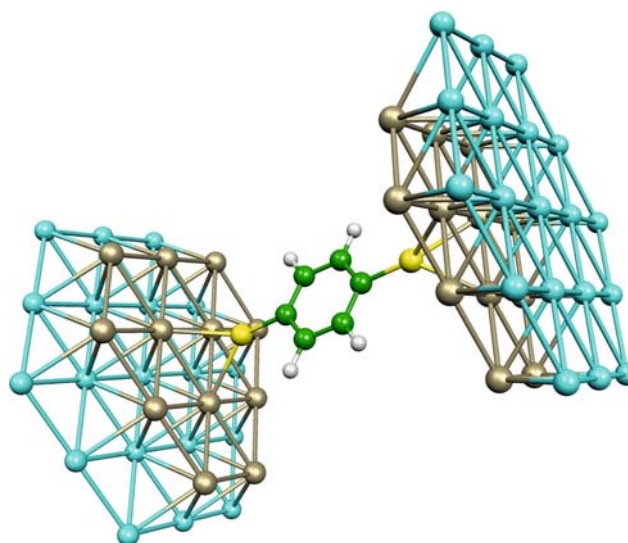


**Fig. 1** The two-layer cluster used in some of the  $I-V$  calculations. The 19 bottom layer Au atoms (colored blue in the online version) use the LanI1 minimal basis set while the top layer atoms use either minimal or double zeta atoms

to model the Au(111) surfaces are taken from the bulk. For the six Au atom chain, the positions of the six Au atoms in the chain and their height above the surface are optimized with the assumption that the chain atoms are above the threefold hollow. For the benzene-1,4-dithiol system, the geometry of the free benzene-1,4-dithiol, with thiol (SH) end-groups, is optimized at the B3LYP/6-31G\* level of theory [21–23]. After removing the terminal H atoms, the symmetry of the  $-\text{SC}_6\text{H}_4\text{S}-$  subunit is very close to  $D_{2h}$  and we idealize the geometry to produce  $D_{2h}$  symmetry. The  $-\text{SC}_6\text{H}_4\text{S}-$  fragment is connected to two Au(111) surfaces, with the  $C_2$  axis of the molecular fragment perpendicular to the surfaces and the S atoms placed above a threefold hollow at a distance of 1.905 Å above the Au surface.

The metal clusters used to describe the surface are one-layer treatments including 6 or 21 gold atoms and a two-layer  $\text{Au}_{31}(12/19)$  cluster containing 12 Au atoms in the top layer and 19 Au atoms the second layer. The one-layer clusters are the same as used previously [13] and the two-layer cluster is shown in Fig. 1. The extended molecule is coupled to the semi-infinite gold (111) surface with the Au cluster atoms removed, whose effects are included as self-energy operators through a recursive Green's function procedure. (n.b. in the two-layer calculations, only the 19 second layer Au atoms are coupled to the semi-infinite gold (111) surface.) The coupling between the bulk contacts and the extended molecule is determined using a tight-binding approach [11], where cluster atoms and their nearest neighbors are coupled directly to the extended molecule.

Most of the  $I-V$  calculations are performed using the pure BPW91 [24, 25] functional, while a few test calcula-

tions are performed using hybrid [21] functionals, namely the B3LYP [22] or the B3PW91 [21] functionals. The  $\alpha$  and  $\beta$  spin densities are constrained to be equal in the  $I$ – $V$  calculations.

The surface Au atoms are described using the Los Alamos 11 valence electron ECP [26], and denoted Lan1. Two different Au minimal basis sets are used. In the full minimal basis, three primitive functions are used for the s, p, and d orbitals, i.e. (3s3p3d)/[1s1p1d], while in the small minimal basis set, the most diffuse s, p, and d primitives are deleted, that is a (2s2p2d)/[1s1p1d] set. These are the same two sets compared in our previous work [13]. We denote these two minimal basis sets as M2G or M3G to signify if there are two or three Gaussian primitives describing the orbitals. In the two-layer calculations, the same minimal basis set is used for both the layers. The Au chain is also described using the Lan1 ECP and the associated basis set, but with the double zeta (DZ) contraction. The same Lan1/DZ basis set is used for three or all of the top layer atoms in some of the two-layer clusters. In addition to the Lan1/DZ treatment of these top layer atoms, the Los Alamos 19 valence electron ECP, denoted Lan2 [27], is used in some two-layer calculations. When benzene-1,4-dithiol is used as the bridging molecule, the C and H are described using the 6-31G\* basis, while S uses the 6-31+G\* basis set [23]. The hybrid integration scheme is used and the C 1s, S 1s, 2s and 2p, and Au 3s and 3p orbitals (when the Lan2 ECP is used) are considered as core orbitals. We use a temperature of 0K for the Au chain and 300K for benzene-1,4-dithiol in the Green's function calculations. The DFT parts of the calculations are performed using Gaussian 03 [28], while all of the Green's function parts are performed using the code described previously [1, 13, 15–19].

For each choice of cluster size and Au basis set, a shift is optimized to eliminate any charging of the bare cluster. The shift is larger for the M3G basis set than the M2G set, for example for the Au<sub>6</sub> cluster the values are 0.1457 and  $-0.0456E_h$ , respectively. However, the shift varies only slightly with cluster size, for example for Au<sub>6</sub> and Au<sub>21</sub> using the M3G basis set the shifts are 0.1457 and 0.1486  $E_h$ , respectively. This shift is then used in the  $I$ – $V$  calculations with the bridging molecule. Clearly the shift is independent of the bridging molecule. Note that for the two-layer clusters, the charge on the entire cluster is eliminated, but there can be some charge separation between the layers, especially if two different basis sets are used.

### 3 Results and Discussion

#### 3.1 The Au<sub>6</sub> chain

In Fig. 2 we plot the results obtained for the M2G Au<sub>6</sub> and Au<sub>31</sub>(12/19) cluster models of the surface using pure and

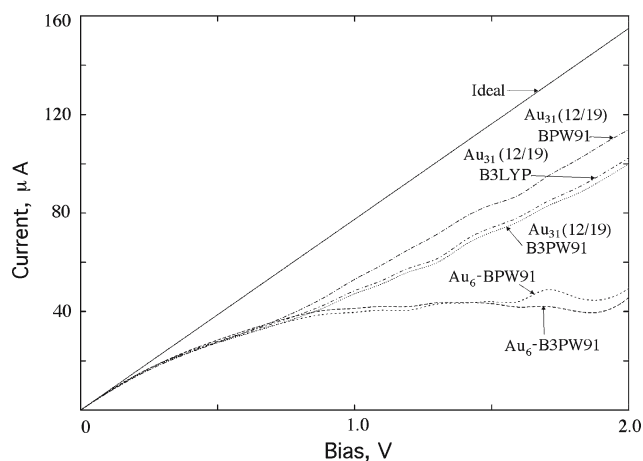


**Fig. 2** A comparison of the pure and hybrid functionals for the Au<sub>6</sub> chain. The M2G basis set is used for the surface Au atoms, while the six Au chain atoms use the Lan1 DZ basis set

hybrid functionals. The ideal (as given by the quantum of conductance)  $I$ – $V$  curve is also plotted to show the theoretical maximum for a single channel. All of the computed  $I$ – $V$  curves are similar up to a bias of about 0.7 V. The hybrid functionals yield a slightly smaller current than the pure BPW91 functional, but the difference is not very large; the differences are especially small for the Au<sub>6</sub> cluster. For the Au chain, the hybrid and pure functionals yield results that are more similar than those found previously for benzene-1,4-dithiol [20] between two Au(111) surfaces. It is also interesting to note that using the hybrid functional lowers the current for both the Au chain and for benzene-1,4-dithiol, but for the benzene-1,4-dithiol this improves agreement with experiment, while for the Au chain this makes the results in poorer agreement with the ideal case. This suggests that if one is testing functionals for the calculation of  $I$ – $V$  curves a variety of systems should be used before drawing any definitive conclusions about the quality of a given functional for the calculation of  $I$ – $V$  curves.

In Fig. 3 we plot the BPW91 results for Au<sub>31</sub>(12/19), Au<sub>21</sub>, and Au<sub>6</sub> using the two different minimal basis sets. For the M2G basis set, the Au<sub>6</sub> cluster yields the smallest current, while the Au<sub>31</sub>(12/19) cluster yields the largest. Compared with the M2G basis set, using the M3G basis set significantly increases the current for the Au<sub>6</sub> cluster, increases the Au<sub>21</sub> cluster results, and decreases the current for the Au<sub>31</sub>(12/19) cluster. It is interesting to note that using the M3G basis set improves the results for the two one-layer clusters, but degrades the two-layer Au<sub>31</sub>(12/19) results. Excluding the Au<sub>6</sub> M2G results, there is reasonable agreement among the different basis sets and different clusters.

In Fig. 4 we compare our Au<sub>31</sub>(12/19) results with calculations where the central three Au atoms (i.e. those closest to the chain) use the Lan1 DZ basis set. These two DZ calculations differ in the choice of the minimal basis set for the other

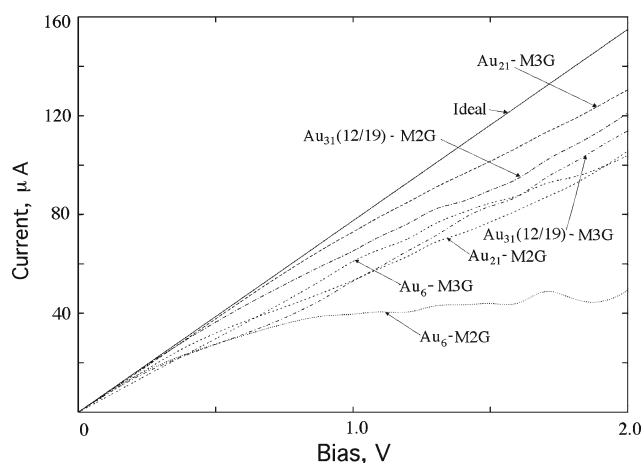


**Fig. 3** A comparison of BPW91 results for the Au<sub>6</sub> chain as a function of basis set and cluster size. The six Au chain atoms use the Lan11 DZ basis set in calculations

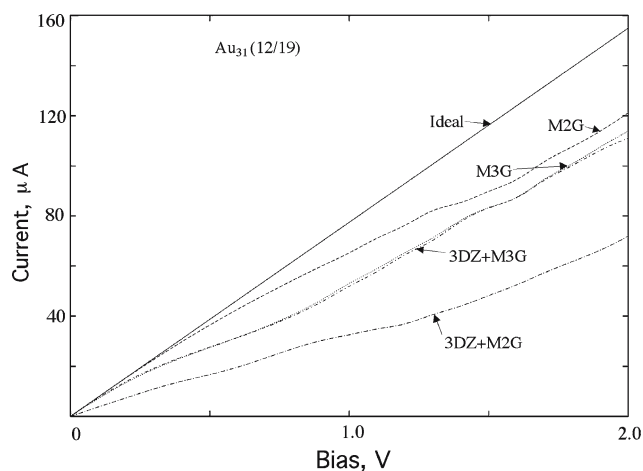


**Fig. 4** A comparison of the Au<sub>6</sub> chain results for the Au<sub>31</sub>(12/19) cluster using 3 DZ(Lan11) atoms in the top layer with the best results obtained using the minimal basis sets for the Au<sub>31</sub> clusters. In the two-layer cluster, the first and second layers use the same minimal basis set, while the six Au chain atoms use the Lan11 DZ basis set

Au atoms. The 3DZ+M3G calculations yields very similar results to the case where all of the Au cluster atoms use M3G basis set. However, the 3DZ+M2G calculations yields significantly smaller currents. Apparently removing the diffuse primitive functions from the minimal basis set, but retaining them on the DZ cluster atoms leads to some imbalance in the basis set that degrades the results.

Overall the results obtained for the Au chain support using either the one-layer Au<sub>21</sub> or the two-layer Au<sub>31</sub>(12/19) cluster with either the M2G or M3G basis set, but for the Au<sub>6</sub> cluster, the M3G set clearly yields superior results. Improving the basis set of the three Au atoms nearest to the Au chain does not significantly improve the results if the M3G set is used for the other Au atoms in the cluster and degrades the result when the M2G basis set is used.

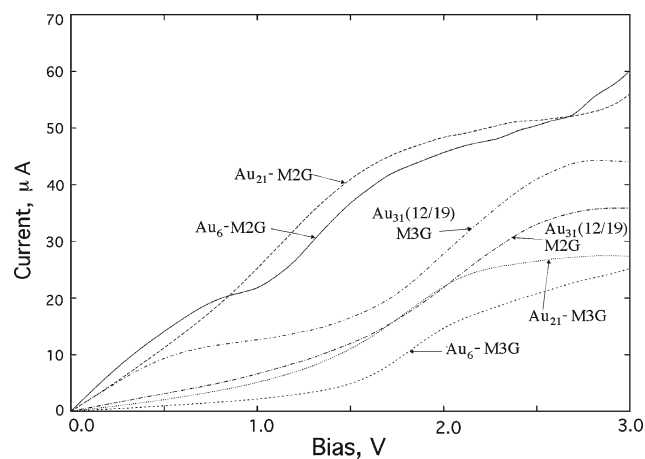


**Fig. 5** The  $I$ – $V$  curves for benzene-1,4-dithiol between two Au(111) surfaces as a function of Au basis set and cluster

### 3.2 benzene-1,4-dithiol

In Fig. 5 we plot the  $I$ – $V$  curves for the Au<sub>6</sub> and Au<sub>21</sub> one-layer clusters and Au<sub>31</sub>(12/19) two-layer cluster using the M3G and M2G minimal basis sets. The computed  $I$ – $V$  curves for this system are about two orders of magnitude larger than the break junction experimental results [29], as is found for all high-level treatments. In this regard, we should note that another experiment [30] finds the conductance to be about two orders of magnitude larger than that found in the break junction experiment. Unfortunately this second experiment does not directly measure the  $I$ – $V$  curves and is performed in solution. The large difference between theory and experiment is also true of other systems studied by several different experimental groups. However, the shape of the  $I$ – $V$  curve for the benzene-1,4-dithiol is similar to those observed for other systems. Therefore, despite the uncertainty in the total current in the experiment of Reed and co-workers [29], we believe that the shape of the experimental  $I$ – $V$  curves is correct and therefore we compare our computed results with the shape of the experimental curve. While the Au<sub>6</sub> and Au<sub>21</sub> M2G results in Fig. 5 are in reasonable agreement with each other, they are not in good agreement with the shape of the experimental curve [29]. (Note that the present Au<sub>6</sub> and Au<sub>21</sub> M2G results differ somewhat from our previously reported values since the shifts are determined for each cluster separately in the present work.) Using the M3G basis set has a dramatic effect on the Au<sub>6</sub> and Au<sub>21</sub>  $I$ – $V$  curves, while the two curves are still similar to each other, both curves now appear more like experiment in shape, namely the current is rather flat near a zero bias and then grows rapidly. For the experiment the growth is near a bias of about 1 V, while in the calculations it occurs near 1.5 V. Note, however, that the current in both computed curves is still about two orders of magnitude larger than in experiment.

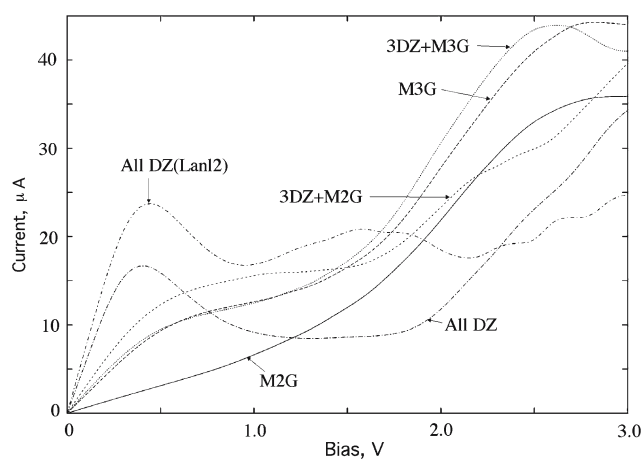


**Fig. 6** The  $I$ – $V$  curves for benzene-1,4-dithiol with the two-layer  $\text{Au}_{31}(12/19)$  cluster

The two-layer  $\text{Au}_{31}(12/19)$  cluster results are somewhat different from the one-layer clusters. The  $\text{Au}_{31}(12/19)$  M2G results are similar to the  $\text{Au}_6$  and  $\text{Au}_{21}$  M3G results. The  $\text{Au}_{31}(12/19)$  current does increase a bit faster than for the one-layer clusters, but it is clear that the  $\text{Au}_{31}(12/19)$  M2G results are more similar to the  $\text{Au}_6$  and  $\text{Au}_{21}$  M3G results than to the  $\text{Au}_6$  and  $\text{Au}_{21}$  M2G results. Using the M3G basis set in conjunction with the two-layer  $\text{Au}_{31}(12/19)$  cluster makes the computed  $I$ – $V$  curve less like experiment, since it has an initial rapid increase in current with bias for small biases. However, the  $\text{Au}_{31}(12/19)$  M3G curve levels out and by about 1 V looks more like the  $\text{Au}_6$  and  $\text{Au}_{21}$  M3G results than the  $\text{Au}_6$  and  $\text{Au}_{21}$  M2G results. These calculations show some of the same trends as observed for the  $\text{Au}_6$  chain, namely the  $\text{Au}_6$  and  $\text{Au}_{21}$  results improve with the basis set is changed from M2G to M3G, while the  $\text{Au}_{31}(12/19)$  results appear to be degraded by the same basis set change.

In Fig. 6 we compare the M2G and M3G results for the two-layer  $\text{Au}_{31}(12/19)$  cluster with those obtained by replacing some or all of the top layer Au atoms with a DZ contraction. Using the DZ/Lan11 valence description for the three Au atoms closest to the S atom with the remaining 9 surface and 19 second layer Au atoms using M3G contraction (3DZ+M3G) yields an  $I$ – $V$  curve very similar to the M3G case, which is similar to the case of the  $\text{Au}_6$  chain. Using the M2G basis set in conjunction with three Lan11 DZ atoms (3DZ+M2G) yields a curve that rises a bit faster at low biases and then falls below the M3G and 3DZ+M3G curves at about 1.5 V. Using the Lan11 DZ basis for all of the top layer Au atoms and the M2G for the second layer (All DZ) yields an  $I$ – $V$  curve that is very strange, rising very rapidly in the 0–0.5 V range then dropping significantly, remaining very flat till 2 V and then rising again.

It is known that the Lan11 approach removes the node in the 6s orbital and hence affects the 5d–6s exchange energy.

Using the Lan12 approach adds the 5s orbital to the valence space and corrects many of the problems found in the Lan11 approach. Replacing all of the top layer atoms with a DZ Lan12 ECP description of the Au atoms (keeping the second layer as M2G) yields an  $I$ – $V$  curve that is as strange as the all DZ(Lan11) results. The fact that the three DZ atom result appears superior to the all DZ atoms is probably related to polarization of charge for the “edge” Au atoms, which is expected to be smaller for case with the minimal basis set since the basis set allows less polarization of these atoms. This problem of the edge atoms is similar to the problem of using the full minimal basis set on the edge atoms in the single layer treatments [13].

It is rather disappointing that using 3DZ atoms does not lead to any improvement and that using all DZ atoms yields very strange result. As previously noted, without any shift the M3G basis set has a much larger charging of the cluster than the M2G set. With this in mind, we modified the DZ basis by scaling the outermost s, p, and d exponents by 1.5 and recontracting the basis set. This change, however, did not significantly affect the results, suggesting that the problems associated with the DZ basis sets is not due to the diffuseness of the basis set. In addition, we should note that part of the problem with using DZ basis set could be due to the formation of a dipole moment since the two layers are treated differently. Thus while adding the shift removes the charging it does not eliminate any polarization of the charge between the layers. However, considering the approximate nature of the shift, it did not seem worthwhile trying to impose other constraints to improve the two layer results.

### 3.3 Transmission

Expanding the cluster from  $\text{Au}_6$  to  $\text{Au}_{21}$  and expanding the basis set from M2G to M3G brings the computed  $I$ – $V$  curves into better agreement with experiment for benzene-1,4-dithiol and into better agreement with the ideal case for the  $\text{Au}_6$  chain. The improvement in the description of the  $I$ – $V$  curves with basis set expansion can be quite dramatic. It is interesting to determine the origin of these changes, and in this regard, we plot the zero bias transmission coefficient for  $\text{Au}_6$  and  $\text{Au}_{21}$  clusters for the  $\text{Au}_6$  chain and benzene-1,4-dithiol, see Fig. 7. The Fermi level has been shifted to 0 eV. We first consider the  $\text{Au}_6$  chain, where the best result is obtained for the  $\text{Au}_{21}$  M3G treatment. In this case, the transmission coefficient is smooth and large near the Fermi level. For the M2G basis set, the transmission coefficient is less smooth and while it is large near the Fermi level, there is a significant dip at about 0.5 eV above the Fermi level. For the  $\text{Au}_6$  cluster, the result obtained using the M3G basis set is smoother than the  $\text{Au}_{21}$  M2G calculation, but not as smooth as the  $\text{Au}_{21}$  M3G result. The  $\text{Au}_6$  M2G result is clearly different from all of

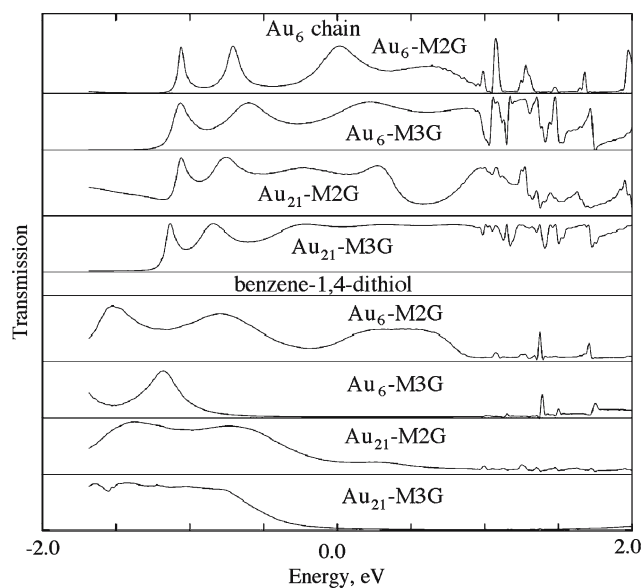


**Fig. 7** Zero bias transmission coefficient for  $Au_6$  and  $Au_{21}$  clusters for the  $Au_6$  chain and benzene-1,4-dithiol. The Fermi level has been shifted to 0 eV

the other curves, which is consistent with the small current obtained using this treatment.

Turning to the benzene-1,4-dithiol case; the  $Au_{21}$  M3G transmission curve is flat from about  $-1.5$  to  $-0.7$  eV, then it decreases to a very small value. The  $Au_{21}$  M2G is similar, except for the plateau that raises the value from about  $-0.7$  to  $0.5$  eV. This increases the transmission coefficient in the region near the Fermi level and leads to the rapid increase in current at small biases in the M2G treatment that is absent in the M3G treatment. The  $Au_6$  M3G approach yields a transmission coefficient close to zero near the Fermi level and hence the slow increase in the current at small biases as observed for the  $Au_{21}$  M3G calculation. However, the small  $Au_6$  cluster results in a single peak at about  $-1.2$  eV, compared with the broad region found for the  $Au_{21}$  cluster; this is probably a result of the small size of the  $Au_6$  cluster. The  $Au_6$  M2G calculation has a bump slightly above the Fermi level that leads to the rapid increase in the current at low biases.

For the two systems studied in this work, increasing the cluster size and improving the basis set tend to eliminate structure in the transmission curves. Associated with these changes is an improvement in the  $I-V$  curves. On this basis, we conclude that our  $Au_{21}$  M3G is our best calculation. We also conclude that the  $Au_6$  M3G calculation is a reasonable level, especially for preliminary calculations.

#### 4 Conclusions

We have tested some extensions to our tight-binding/Green's Functions/DFT approach for the calculation of  $I-V$  curves.

Using the full minimal basis set (M3G), i.e., not deleting the diffuse primitives, requires a large shift to avoid the artificial charging. On the basis of our results for two systems studied, we conclude that the  $Au_{21}$  M3G is our best calculation, despite having to use a larger shift. The  $Au_6$  M3G approach appears to be an excellent compromise between cluster size and accuracy and is a good choice for preliminary calculations or when the  $Au_{21}$  M3G is prohibitively expensive. The use of the M3G basis set for the  $Au_{31}$  (12/19) cluster actually degrades the results relative to the M2G set, suggesting that it would be better to use the M2G basis set for this two-layer cluster. In this regard we note that the  $Au_{31}$  (12/19) M2G results are much more similar to the  $Au_6$  and  $Au_{21}$  M3G results than are the  $Au_{31}$  (12/19) M3G results. While the two-layer is more expensive than the one-layer treatments, it does allow one to study the difference between the threefold hollow with or without an atom in the second layer. Attempts to improve the description of the metal-bridging molecule bonding by using a double zeta contraction of the Au atoms at the adsorption site does not show any significant differences from using the minimal basis set and making all of the atoms in the top layer double zeta results in very strange  $I-V$  curves. At the present time it does not appear that using a two-layer cluster with only the bottom layer coupled to the bulk offers a mechanism of using larger basis sets on the top layer. While adding a shift can be used to eliminate the charging of the cluster, the fact that the two layers in the  $Au_{31}$  (12/19) cluster are treated differently can lead to some charge polarization between the two layers. We would not be surprised if this is the origin of why the  $Au_{31}$  (12/19) behaves differently from the one-layer clusters with respect to the M2G and M3G basis sets, and why improving the basis set on the top layer seems to lead to more problems than it solves.

While the results presented here give some insights into how to improve our treatment, suggesting, for example, that the  $Au_6$  cluster with the M3G basis set may be a superior zeroth order treatment than the  $Au_6$  M2G that we have used in previous work, it is clear that there is still significant room for improvement. In this regard we note that we continue to explore additional methods of improving the treatment of the coupling of the metal clusters to the bulk.

**Acknowledgments** C.W.B is a civil servant in the Space Technology Division (Mail Stop 230-3), while J.W.L. is a civil servant in the TS Division (Mail Stop 229-1).

#### References

- Xue Y, Datta S, Ratner MA (2001) J Chem Phys 115:4292
- Derosa PA, Seminario JM (2001) J Phys Chem B 105:471
- Emberly EG, Kirczenow G (2001) Phys Rev B 64:235412
- Damle P, Ghosh AW, Datta S (2002) Chem Phys 281:171
- Di Ventra M, Pantelides ST, Lang ND (2000) Phys Rev Lett 84:979
- Hall LE, Reimers JR, Hush NS, Silverbrook K (2000) J Chem Phys 112:1510

7. Taylor J, Guo H, Wang J (2001) *Phys Rev B* 63:245407
8. Taylor J, Brandbyge M, Stokbro K (2003) *Phys Rev B* 68:121101(R)
9. Ness H, Shevlin SA, Fisher AJ (2001) *Phys Rev B* 63:125422
10. Magoga M, Joachim C (1997) *Phys Rev B* 56:4722
11. Papaconstantopoulos DA (1986) *Handbook of the band structure of elemental solids*. Plenum, New York
12. Bauschlicher CW, Lawson JW (2007) *Phys Rev B* 75:115406
13. Bauschlicher CW, Xue Y (2005) *Chem Phys* 315:293
14. Lawson JW, Bauschlicher CW (2006) *Phys Rev B* 74:125401
15. Xue Y, Datta S, Ratner MA (2002) *Chem Phys* 281:151
16. Xue Y, Ratner MA (2003) *Phys Rev B* 68:115406
17. Xue Y, Ratner MA (2003) *Phys Rev B* 68:115407
18. Xue Y (2000), PhD thesis, School of Electrical and Computer Engineering, Purdue University, USA
19. Bauschlicher CW, Lawson JW (2006) *Chem Phys* 324:647
20. Bauschlicher CW, Lawson JW, Ricca A, Xue Y, Ratner MA (2004) *Chem Phys Lett* 388:427
21. Becke AD (1993) *J Chem Phys* 98:5648
22. Stephens PJ, Devlin FJ, Chabalowski CF, Frisch MJ (1994) *J Phys Chem* 98:11623
23. Frisch MJ, Pople JA, Binkley JS (1984) *J Chem Phys* 80:3265 and references therein
24. Becke AD (1988) *Phys Rev A* 38:3098
25. Perdew JP, Wang Y (1991) *Phys Rev B* 45:13244
26. Hay PJ, Wadt WR (1985) *J Chem Phys* 82:270
27. Hay PJ, Wadt WR (1985) *J Chem Phys* 82:299
28. Gaussian 03, Revision B05, Frisch MJ, Trucks GW, Schlegel HB, Scuseria GE, Robb MA, Cheeseman JR, Montgomery JA, Vreven T, Kudin KN, Burant JC, Millam JM, Iyengar SS, Tomasi J, Barone V, Mennucci B, Cossi M, Scalmani G, Rega N, Petersson GA, Nakatsuji H, Hada M, Ehara M, Toyota K, Fukuda R, Hasegawa J, Ishida M, Nakajima T, Honda Y, Kitao O, Nakai H, Klene M, Li X, Knox JE, P Hratchian HP, Cross JB, Adamo C, Jaramillo J, Gomperts R, Stratmann RE, Yazyev O, Austin AJ, Cammi R, Pomelli C, Ochterski JW, Ayala PY, Morokuma K, Voth GA, Salvador P, Dannenberg JJ, Zakrzewski VG, Dapprich S, Daniels AD, Strain MC, Farkas O, Malick DK, Rabuck AD, Raghavachari K, Foresman JB, Ortiz JV, Cui Q, Baboul AG, Clifford S, Cioslowski J, Stefanov BB, Liu G, Liashenko A, Piskorz P, Komaromi I, Martin RL, Fox DJ, Keith T, Al-Laham MA, Peng CY, Nanayakkara A, Challacombe M, Gill PMW, Johnson B, Chen W, Wong MW, Gonzalez C, Pople JA (2003) Gaussian, Inc, Pittsburgh
29. Reed MA, Zhou C, Muller CJ, Burgin TP, Tour TM (1997) *Science* 278:252
30. Xiao X, Xu B, Tao NJ (2004) *Nano Lett* 4:267